Available online at www.sciencedirect.com
SCIENCE DIRECT®
Coordination Chemistry Reviews 250 (2006) 259–272
COORDINATION CHEMISTRY REVIEWS
www.elsevier.com/locate/ccr

Review

Group 4 metallocenes incorporating constrained-geometry carboranyl ligands

Zuowei Xie *

Department of Chemistry, The Chinese University of Hong Kong, Shatin NT, Hong Kong, China

Received 15 December 2004; accepted 13 May 2005
Available online 1 July 2005

Contents

Abstract

Ligand modifications have played a crucial role in developing new catalyst precursors for optimizing polymerization activity as well as polymer properties. *o*-Carborane is a highly versatile molecule and can be converted into the *closo*-$C_2B_{10}H_{10}^{2-}$, *nido*-$C_2B_9H_{11}^{2-}$, *nido*-$C_2B_{10}H_{12}^{2-}$, and *arachno*-$C_2B_{10}H_{12}^{4-}$ ligands which are capable of being bonded to metal ions in σ-, η^5-, η^6-, and η^7-fashion, respectively. Such unique features make the replacement possible of either a cyclopentadienyl or an amido unit in the traditional CpSiN constrained-geometry ligands, by a carboranyl moiety. These modifications lead to a novel class of constrained-geometry ligands bearing a carboanion functionality and to a new version of constrained-geometry ligand frameworks incorporating a dicarbollyl moiety. These ligands provide interesting opportunities for the design of metallocenes with new metal/charge and π/σ component combinations and for the study of the role of carborane in catalysis. Achievements, problems and perspectives in this new and rapidly growing field are discussed in this article.

Keywords: Carborane; Catalyst; Cyclopentadienyl; Group 4 metal; Insertion; Metallacarborane; Metallocene; Olefin; Polymerization

1. Introduction

Ligand modifications have played a crucial role in developing new catalyst precursors for optimizing polymerization activity as well as polymer properties, such as stereoregularity, molecular weight, bulky and polar comonomer incorporation, and microstructure [1]. It has been documented that a ligand containing bifunctional groups often offers complexes with some additional advantage [2]. Recently developed constrained-geometry ligands containing both monocyclopentadienyl and σ-heteroatom components have attracted considerable attention [3]. Group 4 metallocenes derived from these ligands are very active catalysts (so called constrained-geometry catalyst (CGC)) for the copolymerization of ethylene with α-olefins due to the increased electron-deficiency and more open coordination environment of the central metal ions by displacing one Cp^-

* Tel.: +852 26096269; fax: +852 26035057.
E-mail address: zxie@cuhk.edu.hk.

0010-8545/$ – see front matter © 2005 Elsevier B.V. All rights reserved.
doi:10.1016/j.ccr.2005.05.009

Table 1
Selected structural data of metallocenes with constrained-geometry carboranyl ligands

Compound	M–X (length, Å)		X–M–X′ (angle, °)		Ref.
[η^5:σ-$Me_2C(C_5H_4)(C_2B_{10}H_{10})$]$Ti(NMe_2)_2$	Ti–C (ring)	2.369 (3)	Cent–Ti–C (cage)	105.0	[15]
	Ti–C (cage)	2.209 (2)	N–Ti–N	106.1 (2)	
	Ti–N	1.894 (2)	C (ring)–C–C (cage)	108.5 (2)	
[η^5:σ-$Me_2C(C_5H_4)(C_2B_{10}H_{10})$]$TiCl(NMe_2)$	Ti–C (ring)	2.341 (2)	Cent–Ti–C (cage)	105.7	[15]
	Ti–C (cage)	2.179 (2)	C (ring)–C–C (cage)	108.5 (2)	
	Ti–N	1.862 (2)	Cl–Ti–N	113.4 (1)	
	Ti–Cl	2.277 (1)			
[η^5:σ-$Me_2C(C_5H_4)(C_2B_{10}H_{10})$]$Zr(NMe_2)_2$	Zr–C (ring)	2.510 (3)	Cent–Zr–C (cage)	100.3	[15]
	Zr–C (cage)	2.343 (3)	N–Zr–N	113.1 (2)	
	Zr–N	2.024 (3)	C (ring)–C–C (cage)	110.7 (2)	
[η^5:σ-$Me_2Si(C_5H_4)(C_2B_{10}H_{10})$]$Zr(NMe_2)_2$	Zr–C (ring)	2.519 (5)	Cent–Zr–C (cage)	108.4	[15]
	Zr–C (cage)	2.353 (4)	N–Zr–N	110.6 (2)	
	Zr–N	2.015 (4)	C (ring)–Si–C (cage)	105.2 (2)	
[η^5:σ-$Me_2Si(C_5H_4)(C_2B_{10}H_{10})$]$Zr(NEt_2)_2$	Zr–C (ring)	2.543 (2)	Cent–Zr–C (cage)	107.6	[15]
	Zr–C (cage)	2.384 (2)	N–Zr–N	110.1 (1)	
	Zr–N	2.031 (2)	C (ring)–Si–C (cage)	104.7 (1)	
[η^5:σ-$Me_2C(C_9H_6)(C_2B_{10}H_{10})$]$Ti(NMe_2)_2$	Ti–C (ring)	2.391 (3)	Cent–Ti–C (cage)	105.4	[15]
	Ti–C (cage)	2.196 (3)	N–Ti–N	104.5 (2)	
	Ti–N	1.896 (3)	C (ring)–C–C (cage)	108.7 (2)	
[η^5:σ-$Me_2C(C_9H_6)(C_2B_{10}H_{10})$]$Zr(NMe_2)_2$	Zr–C (ring)	2.521 (8)	Cent–Zr–C (cage)	101.6	[15]
	Zr–C (cage)	2.326 (7)	N–Zr–N	108.0 (3)	
	Zr–N	2.016 (8)	C (ring)–C–C (cage)	109.4 (6)	
[η^5:σ-$Me_2C(C_9H_6)(C_2B_{10}H_{10})$]$Zr(NEt_2)_2$	Zr–C (ring)	2.538 (2)	Cent–Zr–C (cage)	100.6	[15]
	Zr–C (cage)	2.361 (2)	N–Zr–N	106.6 (1)	
	Zr–N	2.030 (2)	C (ring)–C–C (cage)	110.5 (2)	
[η^5:σ-$Me_2Si(C_9H_6)(C_2B_{10}H_{10})$]$Zr(NMe_2)_2$	Zr–C (ring)	2.541 (5)	Cent–Zr–C (cage)	109.9	[15]
	Zr–C (cage)	2.348 (5)	N–Zr–N	107.3 (2)	
	Zr–N	2.019 (4)	C (ring)–Si–C (cage)	104.8 (2)	
[η^5:σ-$Me_2Si(C_9H_6)(C_2B_{10}H_{10})$]$Zr(NEt_2)_2$	Zr–C (ring)	2.561 (4)	Cent–Zr–C (cage)	107.5	[15]
	Zr–C (cage)	2.362 (4)	N–Zr–N	107.6 (2)	
	Zr–N	2.029 (4)	C (ring)–Si–C (cage)	105.0 (2)	
$[Me_3NH][\{\eta^5$:σ-$Me_2C(C_9H_6)(C_2B_{10}H_{10})\}ZrCl(\mu$-$Cl)_{1.5}]_2$	Zr–C (ring)	2.539 (14)	Cent–Zr–C (cage)	98.4	[15]
	Zr–C (cage)	2.367 (12)	C (ring)–C–C (cage)	111.0 (14)	
	Zr–Cl(μ)	2.634 (3)			
	Zr–Cl (terminal)	2.449 (4)			
$\{Li(THF)_2\}\{[\eta^5$:σ-$Me_2C(C_9H_6)(C_2B_{10}H_{10})]ZrCl(\mu$-$Cl)_{1.5}\}_2$	Zr–C (ring)	2.527 (9)	Cent–Zr–C (cage)	99.5	[15]
	Zr–C (cage)	2.375 (9)	C (ring)–C–C (cage)	109.6 (7)	
	Zr–Cl(μ)	2.641 (3)			
	Zr–Cl (terminal)	2.424 (3)			
$[Me_2NH_2][\{\eta^5$:σ-$Me_2Si(C_9H_6)(C_2B_{10}H_{10})\}ZrCl(\mu$-$Cl)_{1.5}]_2$	Zr–C (ring)	2.545 (12)	Cent–Zr–C (cage)	105.4	[15]
	Zr–C (cage)	2.393 (10)	C (ring)–Si–C (cage)	104.1 (4)	
	Zr–Cl (μ)	2.622 (3)			
	Zr–Cl (terminal)	2.401 (3)			
[η^5:σ-$^i Pr_2NB(C_9H_6)(C_2B_{10}H_{10})$]$Zr(NMe_2)_2$	Zr–C (ring)	2.522 (2)	Cent–Zr–C (cage)	103.0	[23]
	Zr–C (cage)	2.345 (2)	N–Zr–N	106.4 (1)	
	Zr–N	2.026 (2)	C (ring)-B-C (cage)	114.0 (2)	
[η^5:σ-$^i Pr_2NP(C_9H_6)(C_2B_{10}H_{10})$]$Ti(NMe_2)_2$	Ti–C (ring)	2.403 (3)	Cent–Ti–C (cage)	110.0	[30]
	Ti–C (cage)	2.208 (3)	N–Ti–N	103.9 (2)	
	Ti–N	1.889 (3)	C (ring)–P–C (cage)	97.7 (1)	
[η^5:σ-$^i Pr_2NP(C_9H_6)(C_2B_{10}H_{10})$]$Zr(NMe_2)_2$	Zr–C (ring)	2.552 (8)	Cent–Zr–C (cage)	106.6	[30]
	Zr–C (cage)	2.354 (8)	N–Zr–N	110.0 (3)	
	Zr–N	2.020 (7)	C (ring)–P–C (cage)	98.7 (3)	
[η^5:σ-$^i Pr_2NP(C_9H_6)(C_2B_{10}H_{10})$]$Hf(NMe_2)_2$	Hf–C (ring)	2.551 (8)	Cent–Hf–C (cage)	107.1	[30]
	Hf–C (cage)	2.354 (8)	N–Hf–N	107.2 (6)	
	Hf–N	2.020 (7)	C (ring)–P–C (cage)	98.1 (6)	

Table 1 (*Continued*)

Compound	M–X (length, Å)		X–M–X′ (angle, °)		Ref.
$[\eta^5{:}\sigma\text{-}^i Pr_2NP(C_9H_6)(C_2B_{10}H_{10})]Hf(NEt_2)_2$	Hf–C (ring)	2.530 (3)	Cent–Hf–C (cage)	106.6	[30]
	Hf–C (cage)	2.330 (3)	N–Hf–N	107.5 (2)	
	Hf–N	2.012 (3)	C (ring)–P–C (cage)	98.6 (2)	
rac-$[\eta^5{:}\sigma\text{-}Me_2C(C_5H_4)(C_2B_{10}H_{10})]_2Zr$	Zr–C (ring)	2.502 (4)	Cent–Zr–C (cage)	99.5	[11]
	Zr–C (cage)	2.377 (5)	C (ring)–C–C (cage)	110.2	
$[\eta^5{:}\sigma\text{-}Me_2Si(C_5Me_4)(C_2B_{10}H_{10})]TiCl_2$	Ti–C (ring)	2.365 (4)	Cent–Ti–C (cage)	115.4	[13]
	Ti–C (cage)	2.178 (4)	Cl–Ti–Cl	106.0 (1)	
	Ti–Cl	2.234 (1)	C (ring)–Si–C (cage)	102.0 (1)	
$[\eta^5{:}\sigma\text{-}Me_2Si(C_5Me_4)(C_2B_{10}H_{10})]Zr(NMe_2)_2$	Zr–C (ring)	2.544 (5)	Cent–Zr–C (cage)	110.3	[13]
	Zr–C (cage)	2.355 (5)	N–Zr–N	104.5 (2)	
	Zr–N	2.028 (5)	C (ring)–Si–C (cage)	110.3	
$[\eta^5{:}\sigma\text{-}PhHC(C_5H_4)(SC_2B_{10}H_{10})]Ti(NMe_2)_2$	Ti–C (ring)	2.377 (3)	Cent–Ti–S	113.4 (1)	[27]
	Ti–N	1.908 (3)	N–Ti–N	107.3 (1)	
	Ti–S	2.404 (1)	C (ring)–C–C (cage)	118.6 (3)	
$(\eta^5\text{-}C_5Me_5)[\eta^5{:}\sigma\text{-}Me_2C(C_5H_4)(C_2B_{10}H_{10})]TiCl$	Ti–C (Cp* ring)	2.436 (11)	Cent–Ti–C (cage)	101.5	[32]
	Ti–C (Cp ring)	2.383 (10)			
	Ti–C (cage)	2.328 (9)	C (ring)–C–C (cage)	108.8 (7)	
	Ti–Cl	2.347 (3)			
$(\eta^5\text{-}C_5Me_5)[\eta^5{:}\sigma\text{-}Me_2C(C_5H_4)(C_2B_{10}H_{10})]ZrCl$	Zr–C (Cp* ring)	2.538 (9)	Cent–Zr–C (cage)	98.7	[32]
	Zr–C (Cp ring)	2.498 (10)			
	Zr–C (cage)	2.389 (7)	C (ring)–C–C (cage)	109.4 (7)	
	Zr–Cl	2.440 (2)			
$(\eta^5\text{-}C_5Me_5)[\eta^5{:}\sigma\text{-}Me_2C(C_5H_4)(C_2B_{10}H_{10})]HfCl$	Hf–C (Cp* ring)	2.517 (13)	Cent–Hf–C (cage)	99.2	[32]
	Hf–C (Cp ring)	2.493 (13)			
	Hf–C (cage)	2.364 (1)	C (ring)–C–C (cage)	109.1 (9)	
	Hf–Cl	2.418 (3)			
$[\eta^1{:}\eta^5\text{-}(Me_2NCH_2)_2(C_2B_9H_9)]Ti(NMe_2)_2$	Ti–C (cage)	2.432 (5)	Cent–Ti–N (bridge)	97.7	[34]
	Ti–N	1.895 (4)	N–Ti–N	99.8 (2)	
			C (cage)–C–N (bridge)	107.0	
$[\eta^1{:}\eta^5\text{-}(Me_2NCH_2)(C_2B_9H_{10})]_2Zr$	Zr–C (cage)	2.522 (4)	Cent (cage)–Zr–Cent (cage)	138.1	[35]
	Zr–N	2.474 (3)	C (cage)–C (bridge)–N	108.3 (3)	
$(\eta^5\text{-}C_5Me_5)[\eta^1{:}\eta^5\text{-}OCH(Me)(C_2B_9H_{10})]Ti$	Ti–C (ring)	2.373 (9)	Cent (Cp*)–Ti–Cent (cage)	145.6	[39]
	Ti–C (cage)	2.784 (6)	Cent (cage)–Ti–O	106.4	
	Ti–O	1.879 (7)	B (cage)–C (bridge)–O	96.0 (9)	
$(\eta^5\text{-}C_2B_9H_{11})(\eta^5{:}\eta^1\text{-}C_5Me_4CH_2)Ti$	Ti–C (ring)	2.289 (3)	Cent (Cp*)–Ti–Cent (cage)	150.5	[40]
	Ti–C (cage)	2.328 (3)	Ti–C (bridge)–C (Cp^*ring)	64.5 (2)	
	Ti–C (bridge)	2.294 (3)			
$\{[\eta^5{:}\sigma\text{-}Me_2\ Si(C_9H_6)(C_2B_{10}H_{10})]Zr\}_2(\mu\text{-}O)\{\mu\text{-}N[AlMe_2(THF)]\}$	Zr–C (ring)	2.527 (6)	Cent (ring)–Zr–C (cage)	108.3	[41]
	Zr–C (cage)	2.319 (6)	C (ring)–Si–C (cage)	104.8 (2)	
	Zr–N	2.163 (5)	N–Zr–O	84.6 (2)	
	Zr–O	2.201 (5)			
$\{[\eta^5{:}\sigma\text{-}Me_2C(C_9H_6)(C_2B_{10}H_{10})]Zr(NMe_2)\}_2\{\eta^2{:}\eta^2\text{-}(PhC{=}C{=}C{=}CPh)\}$	Zr–C (ring)	2.507 (16)	Cent (ring)–Zr–C (cage)	100.7	[41]
	Zr–C (cage)	2.332 (14)	C (ring)–C–C (cage)	109.6 (12)	
	Zr–N	1.998 (12)			
	Zr–C	2.376 (13)			
$[\{\eta^5{:}\sigma\text{-}Me_2C(C_9H_6)(C_2B_{10}H_{10})\}ZrCl(\eta^3\text{-}C_2B_{10}H_{10})][Li(THF)_4]$	Zr–C (ring)	2.515 (5)	Cent (ring)–Zr–C (cage)	100.4	[42]
	Zr–C (cage)	2.359 (5)	C (ring)–C–C (cage)	109.7 (4)	
	Zr–Cl	2.403 (2)			
	Zr–C (cage′)	2.326 (7)			
$[\eta^5{:}\sigma\text{-}Me_2C(C_9H_6)(C_2B_{10}H_{10})]Zr[N{=}C(Ph)\text{-}NMe_2]_2$	Zr–C (ring)	2.544 (2)	Cent–Zr–C (cage)	100.4	[24]
	Zr–C (cage)	2.359 (2)	C (ring)–C–C (cage)	110.4 (2)	
	Zr–N	1.972 (2)			

Table 1 (*Continued*)

Compound	M–X (length, Å)		X–M–X′ (angle, °)		Ref.
[η^5:σ-Me$_2$C(C$_9$H$_6$)(C$_2$B$_{10}$H$_{10}$)]Zr[N=C-(C$_2$H$_3$)NMe$_2$]$_2$	Zr–C (ring)	2.549 (8)	Cent–Zr–C (cage)	100.4	[24]
	Zr–C (cage)	2.365 (7)	C (ring)–C–C (cage)	110.7 (6)	
	Zr–N	1.974 (7)			
[{η^5:σ-Me$_2$C(C$_9$H$_6$)(C$_2$B$_{10}$H$_{10}$)}Zr(OCH$_3$)(μ-OCH$_3$)]$_2$	Zr–C (ring)	2.539 (1)	Cent–Zr–C (cage)	98.8	[24]
	Zr–C (cage)	2.407 (10)	C (ring)–C–C (cage)	109.7 (9)	
	Zr–O	1.880 (6)			
[{η^5:σ-Me$_2$Si(C$_9$H$_6$)(C$_2$B$_{10}$H$_{10}$)}Zr(OCH$_3$)(μ-OCH$_3$)]$_2$	Zr–C (ring)	2.552 (3)	Cent–Zr–C (cage)	106.3	[24]
	Zr–C (cage)	2.448 (3)	C (ring)–Si–C (cage)	103.7 (1)	
	Zr–O	1.874 (2)			
[η^5:σ-Me$_2$C(C$_9$H$_6$)(C$_2$B$_{10}$H$_{10}$)]Zr(η^2-S$_2$C-NMe$_2$)$_2$	Zr–C (ring)	2.539 (2)	Cent–Zr–C (cage)	99.4	[24]
	Zr–C (cage)	2.388 (3)	C (ring)–C–C (cage)	109.7 (2)	
	Zr–S	2.638 (1)			
[η^5:σ-Me$_2$Si(C$_9$H$_6$)(C$_2$B$_{10}$H$_{10}$)]Zr(η^2-S$_2$C-NMe$_2$)$_2$	Zr–C (ring)	2.558 (5)	Cent–Zr–C (cage)	106.2	[24]
	Zr–C (cage)	2.456 (5)	C (ring)–Si–C (cage)	103.7 (2)	
	Zr–S	2.645 (1)			
[η^5:σ-Me$_2$C(C$_9$H$_6$)(C$_2$B$_{10}$H$_{10}$)]Zr[η^2-OC-(NMe$_2$)NPh]$_2$	Zr–C (ring)	2.541 (4)	Cent–Zr–C (cage)	98.5	[24]
	Zr–C (cage)	2.378 (4)	C (ring)–C–C (cage)	109.5 (3)	
	Zr–N	2.242 (3)			
	Zr–O	2.165 (3)			
[η^5:σ-Me$_2$Si(C$_9$H$_6$)(C$_2$B$_{10}$H$_{10}$)]Zr[η^2-OC-(NMe$_2$)NPh]$_2$	Zr–C (ring)	2.554 (3)	Cent–Zr–C (cage)	105.6	[24]
	Zr–C (cage)	2.414 (2)	C (ring)–Si–C (cage)	104.3 (1)	
	Zr–N	2.227 (2)			
	Zr–O	2.161 (2)			
[η^5:σ-Me$_2$Si(C$_9$H$_6$)(C$_2$B$_{10}$H$_{10}$)]Zr[η^2-OC-(NMe$_2$)NPh][η^2-OC(NMe$_2$)N(Ph)C=(NPh)O]	Zr–C (ring)	2.563 (5)	Cent–Zr–C (cage)	105.7	[24]
	Zr–C (cage)	2.422 (5)	C (ring)–Si–C (cage)	104.3 (2)	
	Zr–N	2.180 (4)			
	Zr–O	2.151 (3)			
[η^5:σ-Me$_2$C(C$_9$H$_6$)(C$_2$B$_{10}$H$_{10}$)]Zr(NMe$_2$)[η^2-SC(NMe$_2$)NBu^n]	Zr–C (ring)	2.532 (2)	Cent–Zr–C (cage)	100.1	[24]
	Zr–C (cage)	2.410 (2)	C (ring)–C–C (cage)	110.1 (2)	
	Zr–N	1.997 (2)			
	Zr–N (imido)	2.268 (2)			
	Zr–S	2.621 (1)			
[η^5:σ-Me$_2$Si(C$_9$H$_6$)(C$_2$B$_{10}$H$_{10}$)]Zr(NMe$_2$)[η^2-SC(NMe$_2$)NBu^n]	Zr–C (ring)	2.571 (6)	Cent–Zr–C (cage)	107.3	[24]
	Zr–C (cage)	2.438 (5)	C (ring)–Si–C (cage)	105.8 (3)	
	Zr–N	1.975 (5)			
	Zr–N (imido)	2.270 (5)			
	Zr–S	2.606 (2)			
[η^5:σ-Me$_2$Si(C$_9$H$_6$)(C$_2$B$_{10}$H$_{10}$)]Zr[η^2-SC-(NMe$_2$)NBu^n]$_2$	Zr–C (ring)	2.559 (10)	Cent–Zr–C (cage)	98.3	[24]
	Zr–C (cage)	2.398 (9)	C (ring)–Si–C (cage)	110.5 (8)	
	Zr–N	2.268 (8)			
	Zr–S	2.578 (3)			

with a RO$^-$, or R$_2$N$^-$, or R$_2$P$^-$ unit [1b,3]. The lone-pair electrons of the heteroatom can form a back bond with the empty d-orbitals of the d^0 group 4 metal ions in addition to the σ bond, which can decrease the Lewis acidity of the metal center and stabilize the (Cp–D)MR$^+$ moiety, probably leading, to some extent, to lower catalytic activity. It is anticipated that a new system with an appended carboanion functionality, this is, the heteroatom unit in the classical constrained-geometry ligands is replaced by a carboanion moiety, may have a higher activity in olefin polymerization by eliminating the back bonding interactions. On the other hand, replacement of a uninegative C$_5$R$_5^-$ moiety in the classical constrained-geometry ligands by an isolobal, dinegative dicarbollide one (C$_2$B$_9$H$_{11}^{2-}$) reduces the overall charge of the resulting metallocenes by one unit but leaves the gross structural and metal frontier orbital properties unchanged. Such a new metal/charge combination would have a high impact on the catalytic activity of metallocenes. This review summarizes the development in metallocene catalysts incorporating constrained-geometry carboranyl ligands of the types [L(C$_5$R$_4$)(C$_2$B$_{10}$H$_{10}$)]$^{2-}$, [L(C$_9$H$_6$)(C$_2$B$_{10}$H$_{10}$)]$^{2-}$, [(CH$_2$)$_n$N(R)(C$_2$B$_9$H$_{10}$)]$^{3-}$, [(CH$_2$)$_n$N(R$_2$)(C$_2$B$_9$H$_{10}$)]$^{2-}$,

Table 2
Ethylene polymerization results

Catalyst	Al/M	T_p (°C)	Activity (10^4 g PE mol^{-1} h^{-1} atom^{-1})	T_m (°C)	Reference
[Me_3NH] [{η^5:σ-Me_2 C(C_9H_6)(C_2 $B_{10}H_{10}$)}$ZrCl(\mu$-Cl) $_{1.5}]_2$	1500	60	334	130.5	[15]
{$Li(THF)_2$}{[η^5:σ-$Me_2C(C_9H_6)(C_2B_{10}H_{10})$]$ZrCl(\mu$-Cl)$_{1.5}\}_2$	1500	60	273	131.2	[15]
[Me_2NH_2] [{η^5:σ-Me_2 Si(C_9H_6)(C_2 $B_{10}H_{10}$)}$ZrCl(\mu$-Cl)$_{1.5}]_2$	1500	60	261	129.8	[15]
[Me_3NH][{η^5: σ-$Me_2Si(C_9$ H_6)(C_2 $B_{10}H_{10}$)} $ZrCl(\mu$-Cl)$_{1.5}]_2$	1500	60	291	129.5	[15]
[η^5:σ-^{i} $Pr_2NB(C_9$ H_6)(C_2 $B_{10}H_{10}$)] $Zr(NMe_2)_2$	1500	25	20	135.5	[23]
[η^5:σ-^{i}Pr_2 $NB(C_9H_6)$ (C_2B_{10} H_{10})]$TiCl_2$	1500	25	7	131.3	[23]
[η^5:σ-^{i}Pr_2 $NB(C_9H_6)$ ($C_2B_{10}H_{10}$)] $ZrCl_2$	1500	25	350	137.0	[23]
[η^5:σ-^{i}Pr_2NB (C_9H_6) ($C_2B_{10}H_{10}$)] $HfCl_2$	1500	25	3	129.6	[23]
[η^5:σ-^{i}$Pr_2NB(C_9H_6)(C_2B_{10}H_{10})$]$Zr(CH_3)_2$	1500	25	20	130.6	[23]
[η^5:σ-^{i}$Pr_2NP(C_9H_6)(C_2B_{10}H_{10})$]$Zr(NMe_2)_2$	1500	25	0.4		[30]
(η^5-C_5Me_5)[η^5:σ-$Me_2C(C_5H_4)(C_2B_{10}H_{10})$]TiCl	1500	70	0.09	131.7	[32]
(η^5-C_5Me_5)[η^5:σ-$Me_2C(C_5H_4)(C_2B_{10}H_{10})$]ZrCl	1500	70	0.5	134.4	[32]
[η^1:η^5-(Me_2NCH_2)($C_2B_9H_{10}$)]$TiCl_2$	500	40	8.5	129	[35]
[η^1:η^5-(Me_2NCH_2)(Me)($C_2B_9H_9$)]$TiCl_2$	500	40	5.5	131	[35]
[σ:η^5-$Me_2Si(NBu^t)(C_5Me_4)$]$Zr(NMe_2)_2$	890	60	27	122	[33]
[σ:η^5-$H_2C(NBu^t)(C_5Me_4)$]$Zr(NEt_2)_2$	1470	60	97	131	[33]

{[$(CH_2)_nN(R_2)$]$_2(C_2B_9H_9)$]}$^{2-}$, and [$Me_2Si(NR)(C_2B_{10}H_{11})$]$^{3-}$. For easy comparisons, Table 1 lists key structural data of metallocenes bearing the above ligands, and ethylene polymerization results employing these metallocenes/MAO are compiled in Table 2.

2. Metallocenes with linked Cp–carboranyl ligands

2.1. Ligand synthesis

To prepare constrained-geometry ligands with a carboanion functionality is a very challenging project since carboanions: (1) are very reactive; (2) should not contain any β-H atoms; (3) must be sterically demanding to prevent the M–C bond from the attack of olefins in catalysis. In this connection, the icosahedral *o*-carborane is an ideal molecule because its cage C–H is readily deprotonated by *n*-BuLi to form the corresponding thermally stable and very bulky dilithium salt [$C_2B_{10}H_{10}$]Li_2 with no β-H atoms [4]. The target molecules were realized by coupling cyclopentadienyl and carboranyl moieties. For example, treatment of [$C_2B_{10}H_{10}$]Li_2 with (C_5H_5)$SiMe_2Cl$ in toluene/ether gave, after hydrolysis, a linked cyclopentadienyl–carboranyl compound $Me_2Si(C_5H_5)(C_2B_{10}H_{11})$ [5] as shown in Scheme 1. A dilithium salt must be used since one molar equivalent is consumed by the acidic proton of cyclopentadiene in (C_5H_5)$SiMe_2Cl$ and the remaining one is necessary to provide the nucleophile for reaction with Si–Cl bond to form the target molecule. Thus, following this motif, a new class of linked cyclopentadienyl (or indenyl, or fluorenyl)–carboranyl compounds can be prepared via nucleophilic substitution reaction of $Li_2C_2B_{10}H_{10}$ with different electrophiles in which both the nature of the electrophilic site and the structure of the cyclopentadienyl ring can be varied [6–28]. Some examples are listed in Fig. 1.

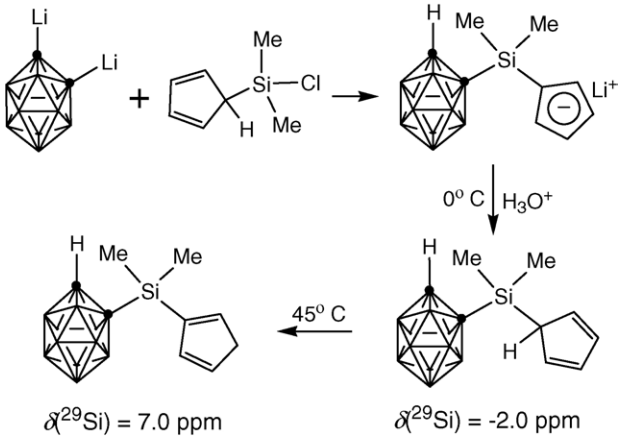

Scheme 1.

2.2. Metallocenes

There are two general methods to prepare group 4 metallocenes: salt metathesis and amine (or alkane) elimination. The two acidic protons, cage CH and sp^3-CH from the five-membered ring, in linked compounds shown in Fig. 1 make the amine elimination reaction of the ligands with metal amides possible. For instance, treatment of $M(NR_2)_4$ (M = group 4 metals; R = Me, Et; except for $Ti(NEt_2)_4$) with one equivalent of $Me_2A(C_9H_7)(C_2B_{10}H_{11})$ or $Me_2A(C_5R_4H)(C_2B_{10}H_{11})$ (A = C, Si) in toluene at reflux temperature gave the corresponding group 4 metal amides of the general formula [η^5:σ-$Me_2A(C_9H_6)(C_2B_{10}H_{10})$]$M(NR_2)_2$ (Scheme 2) and [η^5:σ-$Me_2A(C_5R_4)(C_2B_{10}H_{10})$]$M(NR_2)_2$ (Scheme 3), respectively, in good isolated yields [15]. A longer reaction time causes growth of intense color of the resulting solution and a lower isolated yield. Under the same reaction conditions, $Ti(NEt_2)_4$ did not react with any one of the

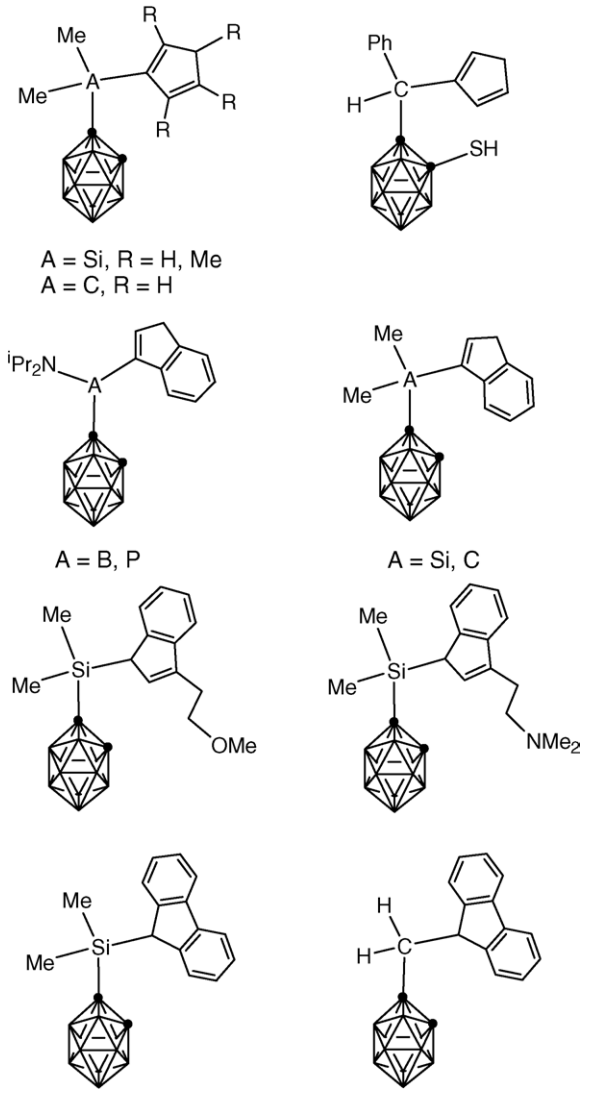

Fig. 1. Linked Cp–carboranyl compounds.

neutral ligands mentioned above probably because of steric effects.

For the ligand containing a SH group, the reaction proceeded at room temperature. Reaction of $Ti(NMe_2)_4$ with

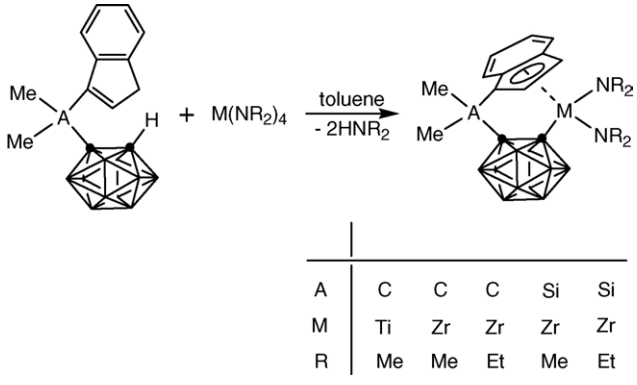

Scheme 2.

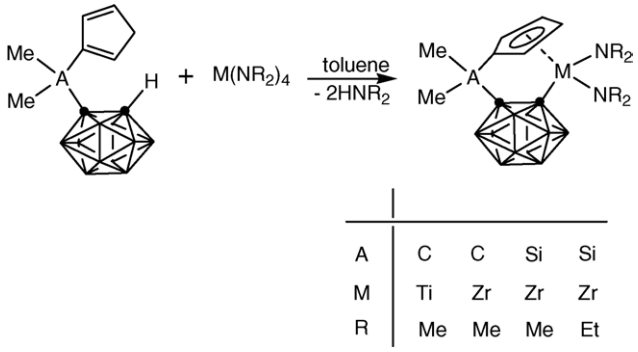

Scheme 3.

one equivalent of $PhHC(C_5H_5)(HSC_2B_{10}H_{10})$ in toluene at 25 °C offered $[\eta^5{:}\sigma\text{-}PhHC(C_5H_4)(SC_2B_{10}H_{10})]Ti(NMe_2)_2$ (Scheme 4) [27].

The representative structures of carbon- and silicon-linked constrained-geometry group 4 metal amide complexes are shown in Figs. 2–4, respectively. The central metal atom is η^5-bound to one five-membered ring of either cyclopentadienyl or indenyl group and σ-bound to a cage carbon atom (or sulfur atom) and two amido groups (NR_2) in a distorted-tetrahedral geometry. The nitrogen atoms are all flat (sum of angles around N ≈360°), which indicates the sp^2 hybridization at N and partial $N(p_\pi) \rightarrow M(d_\pi)$ interactions. The lack of additional electron donation from the carboranyl group to the M center strengthens this $p_\pi \rightarrow d_\pi$ interactions, leading to noticeably shorter M–N bond distances compared with the corresponding M–N bond distances observed in the classical constrained-geometry metallocenes [29].

Amine elimination methodology was also applied to boron- and phosphorus-linked ligands. In general, reactions of $^{i}Pr_2NA(C_9H_7)(C_2B_{10}H_{11})$ with one equivalent of $M(NMe_2)_4$ in toluene at 65–70 °C gave the desired complexes $[\eta^5{:}\sigma\text{-}^{i}Pr_2NA(C_9H_6)(C_2B_{10}H_{10})]M(NMe_2)_2$ (A = B [23], P [30]; M = group 4 metals) in good isolated yields (Schemes 5 and 6). Under the similar reaction conditions, however, interaction between $^{i}Pr_2NB(C_9H_7)(C_2B_{10}H_{11})$ and

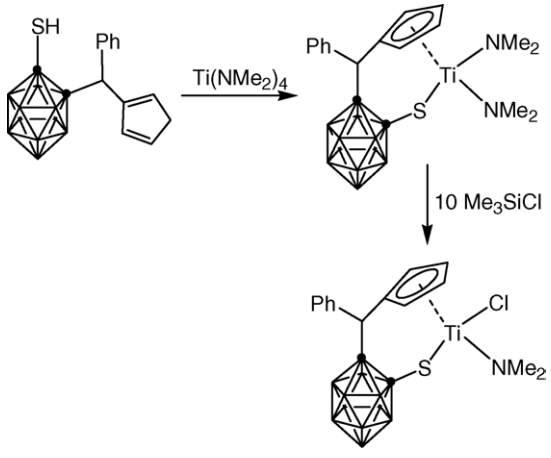

Scheme 4.

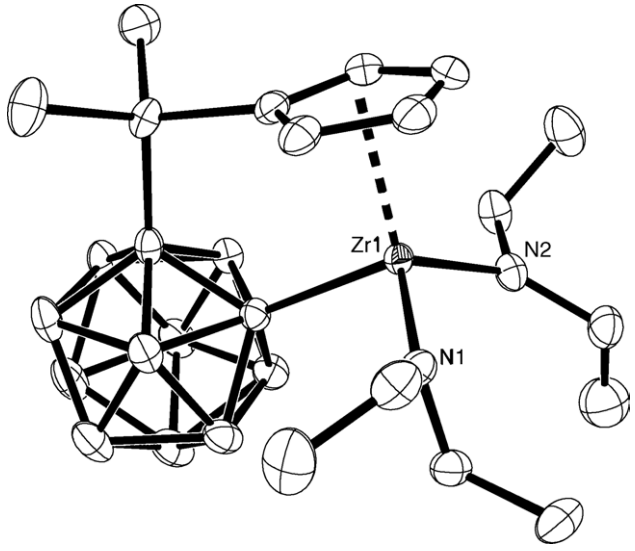

Fig. 2. Molecular structure of $[\eta^5{:}\sigma\text{-}Me_2Si(C_5H_4)(C_2B_{10}H_{10})]Zr(NEt_2)_2$ [15].

an equimolar amount of $Ti(NMe_2)_4$ in toluene did not lead to the isolation of the expected complex $[\eta^5{:}\sigma\text{-}{}^iPr_2NB(C_9H_6)(C_2B_{10}H_{10})]Ti(NMe_2)_2$; instead, the deborated product $(\eta^5\text{-}C_2B_9H_{11})Ti(NMe_2)_2(HNMe_2)$ was isolated in 29% yield. It was assumed that NMe_2^- in $Ti(NMe_2)_4$ might attack the bridging B atom and the cage B atom leading to the formation of this deborated product [23].

There are no reactions between $M(CH_2C_6H_5)_4$ and $Me_2A(C_9H_7)(C_2B_{10}H_{11})$ or $Me_2A(C_5H_5)(C_2B_{10}H_{11})$. These results suggest that acidity or basicity of reactants is not the sole factor to control these acid–base reactions, steric factor may play a role.

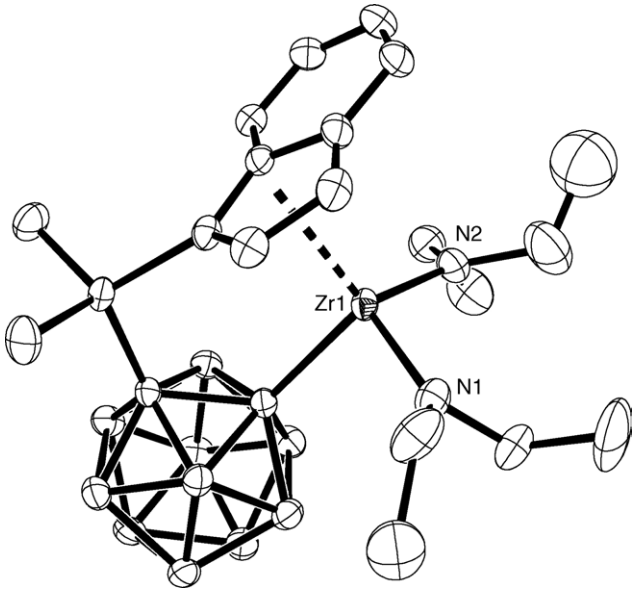

Fig. 3. Molecular structure of $[\eta^5{:}\sigma\text{-}Me_2Si(C_9H_6)(C_2B_{10}H_{10})]Zr(NEt_2)_2$ [15].

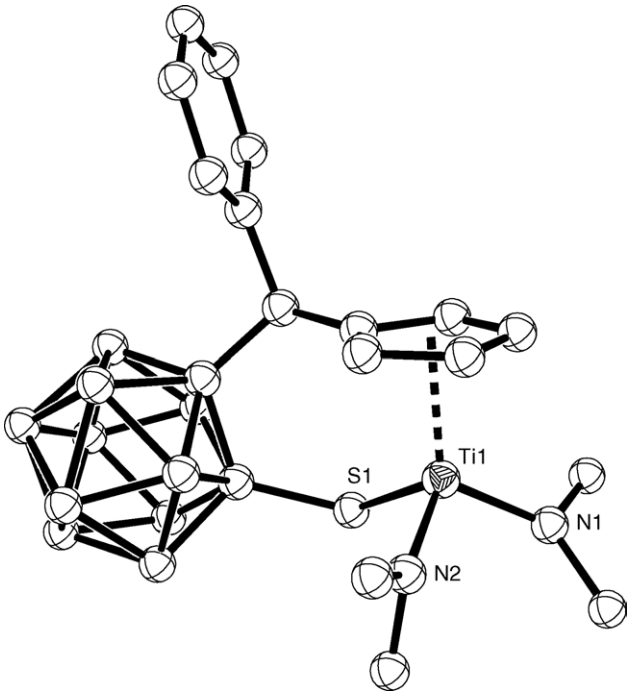

Fig. 4. Molecular structure of $[\eta^5{:}\sigma\text{-}PhHC(C_5H_4)(SC_2B_{10}H_{10})]Ti(NMe_2)_2$ [27].

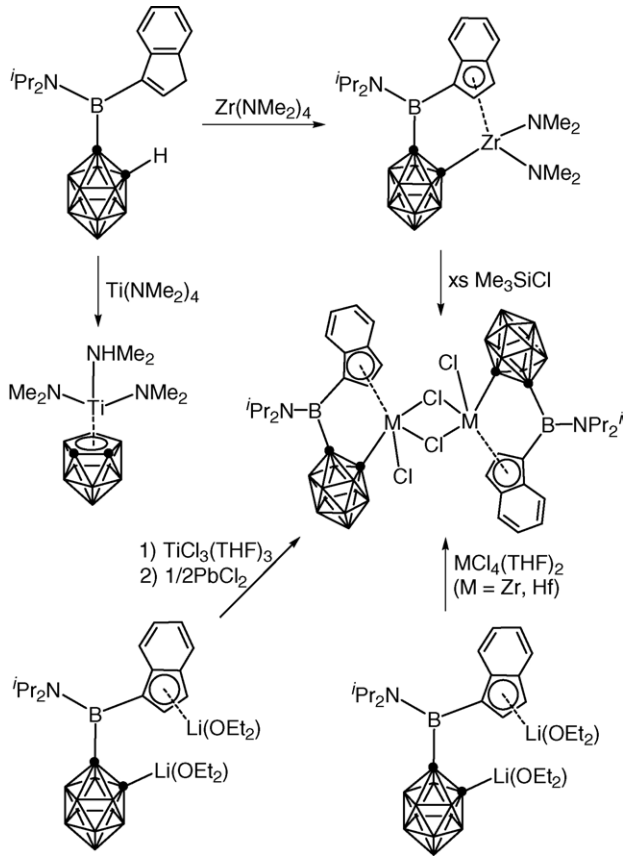

Scheme 5.

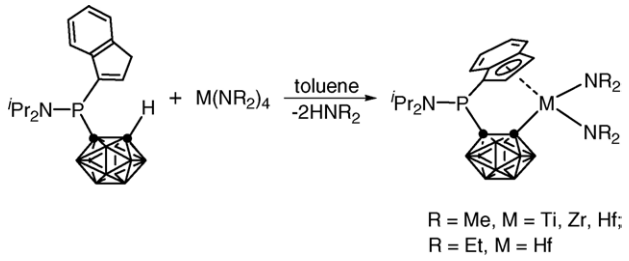

Scheme 6.

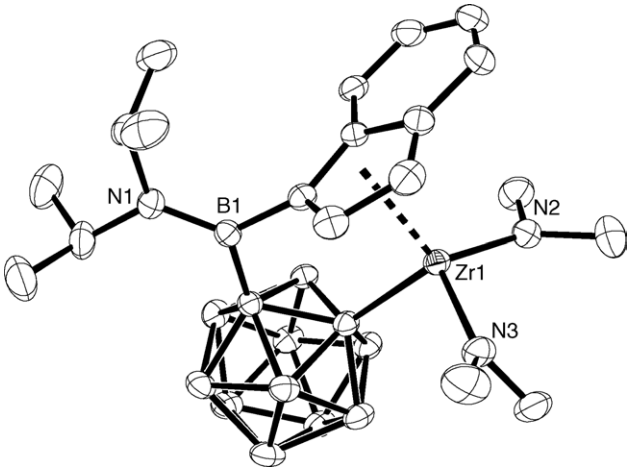

Fig. 5. Molecular structure of $[\eta^5{:}\sigma\text{-}^i Pr_2B(C_9H_6)(C_2B_{10}H_{10})]Zr(NMe_2)_2$ [23].

Figs. 5 and 6 show the representative structures of boron- and phosphorus-linked constrained-geometry group 4 metal amide complexes, respectively. The coordination geometry of the central metal atom is very similar to that observed in

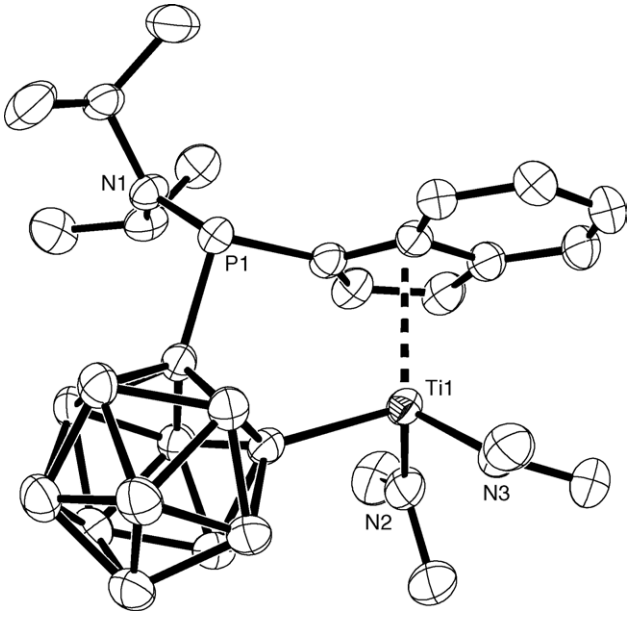

Fig. 6. Molecular structure of $[\eta^5{:}\sigma\text{-}^i Pr_2P(C_9H_6)(C_2B_{10}H_{10})]Ti(NMe_2)_2$ [30].

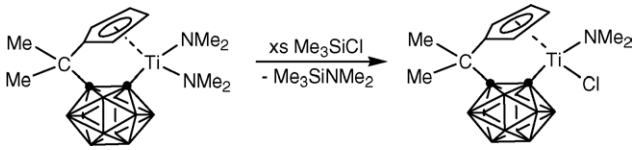

Scheme 7.

the C- and Si-linked analogues. The bridging boron and three nitrogen atoms are all in a trigonal planar environment (sum of angles around N and B ~360°), suggesting the presence of $N(p_\pi) \rightarrow B(p_\pi)$ and $N(p_\pi) \rightarrow M(d_\pi)$ interactions. On the other hand, the bridging phosphorus atom adopts a trigonal-pyramidal coordination geometry owing to the presence of lone-paired electrons.

The above constrained-geometry carboranyl group 4 metal amides can be conveniently converted into the corresponding chloride complexes by interaction with Me_3NHCl or Me_2NH_2Cl or Me_3SiCl dependent upon the ligand systems and group 4 metal ions. For example, reaction of $[\eta^5{:}\sigma\text{-}Me_2C(C_5H_4)(C_2B_{10}H_{10})]Ti(NMe_2)_2$ or $[\eta^5{:}\sigma\text{-}PhHC(C_5H_4)(SC_2B_{10}H_{10})]Ti(NMe_2)_2$ with excess Me_3SiCl in toluene generated the corresponding monochloro metal amides $[\eta^5{:}\sigma\text{-}Me_2C(C_5H_4)(C_2B_{10}H_{10})]TiCl(NMe_2)$ (Scheme 7) [15] or $[\eta^5{:}\sigma\text{-}PhHC(C_5H_4)(SC_2B_{10}H_{10})]TiCl(NMe_2)$ (Scheme 4) [27]. Such a reaction would be a good method for the preparation of chiral metallocenes due to the simple workup procedure and high yield. Treatment of $[\eta^5{:}\sigma\text{-}Me_2A(C_9H_6)(C_2B_{10}H_{10})]Zr(NMe_2)_2$ with 2.5 equivalents of $Me_3N{\cdot}HCl$ afforded $[Me_3NH][\{\eta^5{:}\sigma\text{-}Me_2A(C_9H_6)(C_2B_{10}H_{10})\}ZrCl(\mu\text{-}Cl)_{1.5}]_2$ (A = C, Si) in a typical yield of 85% (Scheme 8) [15]. Surprisingly, the Zr–C (cage) bond remains intact in these reactions even in the presence of excess $Me_3N{\cdot}HCl$, implying that Zr–C (cage) σ bond is well protected by the icosahedral moiety.

Fig. 7 shows the monomeric structure of monochloro metal amide complex. The structural features are similar to its parent amide complex except for the replacement of a NMe_2 group with one chlorine atom. On the other hand, the molecular structures of the dichloro complexes are significantly different from their parent amides. Their solid-state structures consist of alternating layers of discrete cations $[Me_2NH_2]^+$ or $[Me_3NH]^+$ and anions $\{[\eta^5{:}\sigma\text{-}Me_2A(C_9H_6)(C_2B_{10}H_{10})]ZrCl(\mu\text{-}Cl)_{1.5}\}_2^-$. The anion is a dimeric species bearing the $Zr(\mu\text{-}Cl)_3Zr$ moiety. Each Zr atom is η^5-bound to one five-membered ring of indenyl group and σ-bound to a cage carbon atom, one terminal chlorine atom and three doubly bridging chlorine atoms in a distorted-octahedral geometry shown in Fig. 8. They are formally 16-electron complexes. These results indicate that Lewis acidity of the central Zr atom increases greatly after the displacement of NMe_2^- by Cl^- due to the elimination of the $N(p_\pi) \rightarrow Zr(d_\pi)$ interactions.

Group 4 metallocene chlorides were also prepared from the reaction of $MCl_4(THF)_2$ with the dilithium salts of the constrained-geometry carboranyl ligands shown in

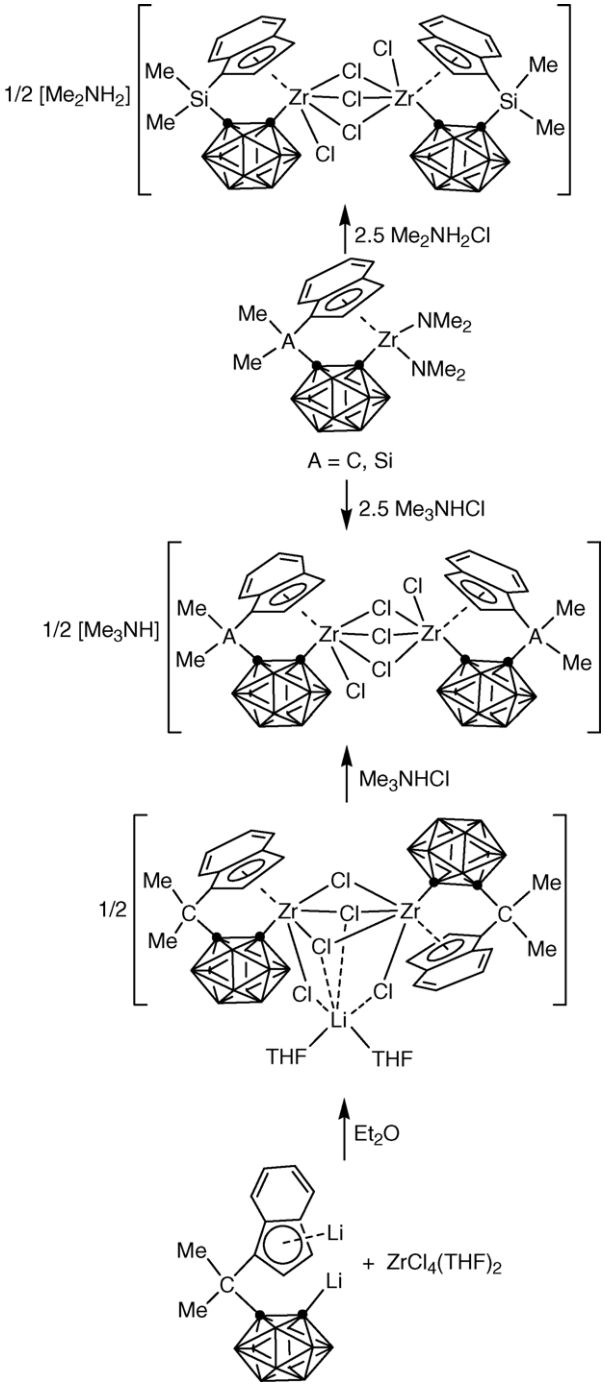

Scheme 8.

Schemes 5 and 8 [15,23]. Both neutral and 'ate' complexes were isolated dependent upon the ligands. A representative structure of the 'ate' complex is illustrated in Fig. 9. The incorporated LiCl was not removable via recrystallization from hot toluene. The Li^+ ion, however, could be displaced by other cations, such as Me_3NH^+ (Scheme 8). In contrast, the titanium analogues were normally prepared from the reaction of $TiCl_3(THF)_3$ with the dilithium salts of the constrained-geometry carboranyl ligands followed by treat-

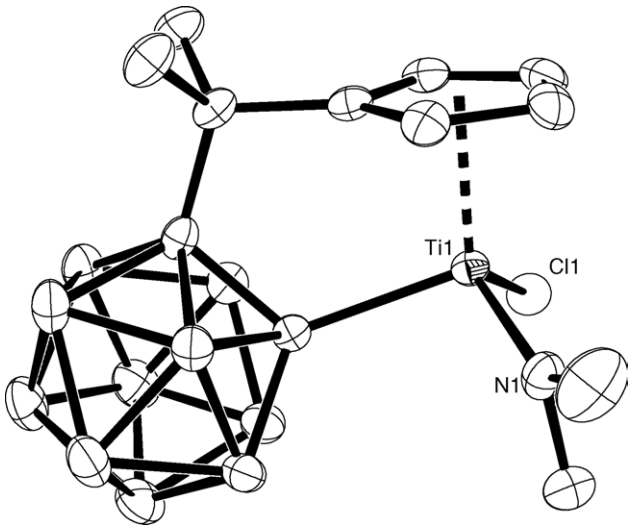

Fig. 7. Molecular structure of $[\eta^5{:}\sigma\text{-}Me_2C(C_5H_4)(C_2B_{10}H_{10})]TiCl(NMe_2)$ [15].

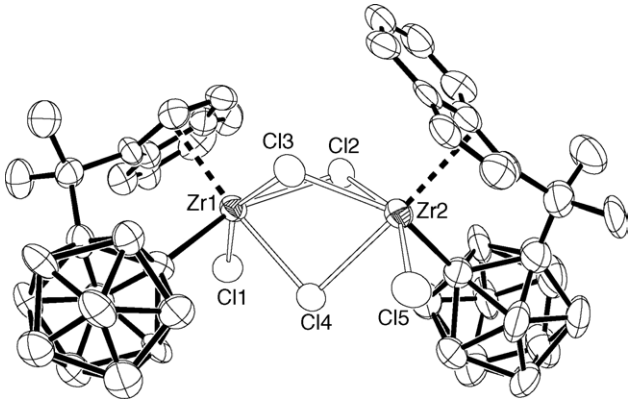

Fig. 8. Molecular structure of the anion $[\{\eta^5{:}\sigma\text{-}Me_2C(C_9H_6)(C_2B_{10}H_{10})\}ZrCl(\mu\text{-}Cl)_{1.5}]_2^-$ [15].

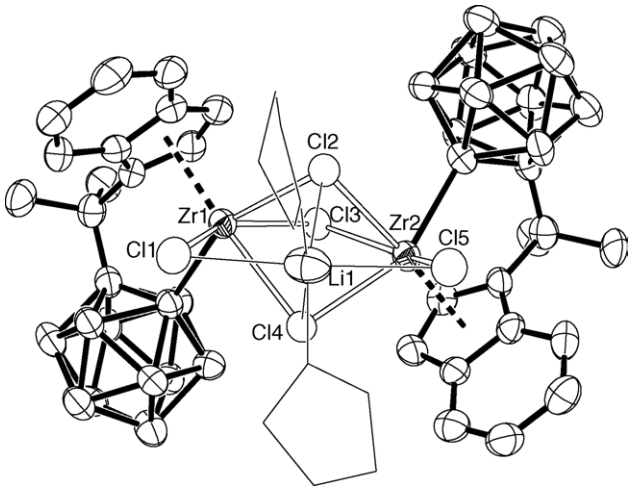

Fig. 9. Molecular structure of $\{[\eta^5{:}\sigma\text{-}Me_2C(C_9H_6)(C_2B_{10}H_{10})]ZrCl(\mu\text{-}Cl)_{1.5}\}_2\{Li(THF)_2\}$ [15].

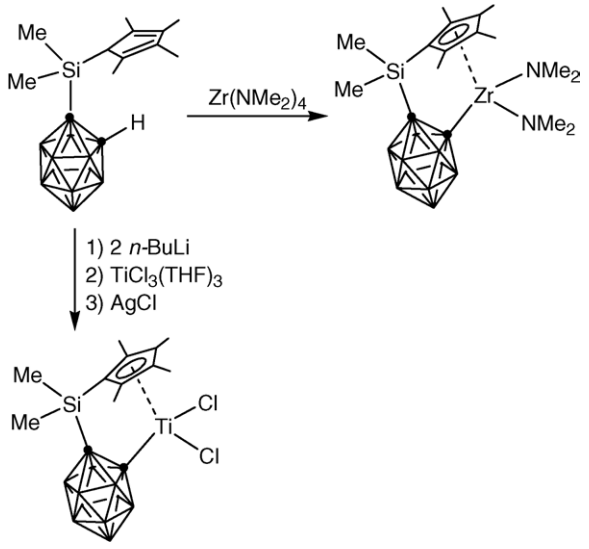

Scheme 9.

ment with $PbCl_2$ [23] (Scheme 5) or AgCl [13] (Scheme 9) since Ti(IV) was often reduced to Ti(III) by lithium reagents [31].

Reaction of $[Me_2C(C_5H_4)(C_2B_{10}H_{10})]Li_2$ with 0.5 equivalent of $ZrCl_4$ or one equivalent of $(C_5Me_5)MCl_3$ (M = group 4 metals) in toluene gave $[\eta^5{:}\sigma\text{-}Me_2C(C_5H_4)(C_2B_{10}H_{10})]_2Zr$ (Scheme 10) [11] or $(\eta^5\text{-}C_5Me_5)[\eta^5{:}\sigma\text{-}Me_2C(C_5H_4)(C_2B_{10}H_{10})]MCl$ (Scheme 10) [32], respectively. Single-crystal X-ray analyses confirmed their monomeric structures. Figs. 10 and 11 show their representative molecular structures.

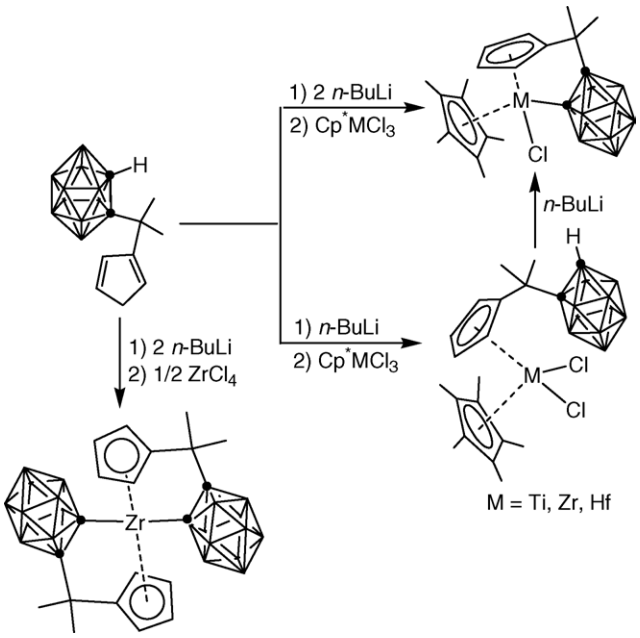

Scheme 10.

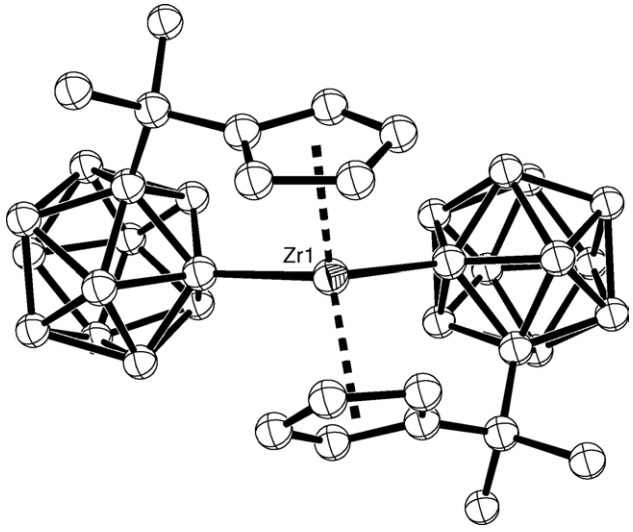

Fig. 10. Molecular structure of $[\eta^5{:}\sigma\text{-}Me_2C(C_5H_4)(C_2B_{10}H_{10})]_2Zr$ [11].

2.3. Polymerization of olefins

Most of metallocenes derived from linked Cp–carboranyl constrained-geometry ligands are active catalysts for polymerization of ethylene with moderate to very high activities (10^3–10^6 g mol^{-1}atom h^{-1}) in the presence of cocatalyst MAO or MMAO. Table 2 summarizes the ethylene polymerization results reported in the literature employing metallocenes with various constrained-geometry carboranyl ligands. The results show that the central metal ions and the linkages of the bridged ligands have a great effect on the catalytic performance of the catalysts, and the following trends are generally observed if other factors are identical: (1) Zr ≫ Ti > Hf and (2) ^{i}Pr$_2$NB > Me$_2$C ∼ Me$_2$Si > ^{i}Pr$_2$NP. Table 2 also indicates that zirconocenes with Me_2C- and Me_2Si-linked indenyl–carboranyl ligands are 30–100 times more active than those with R_2C- and Me_2Si-linked

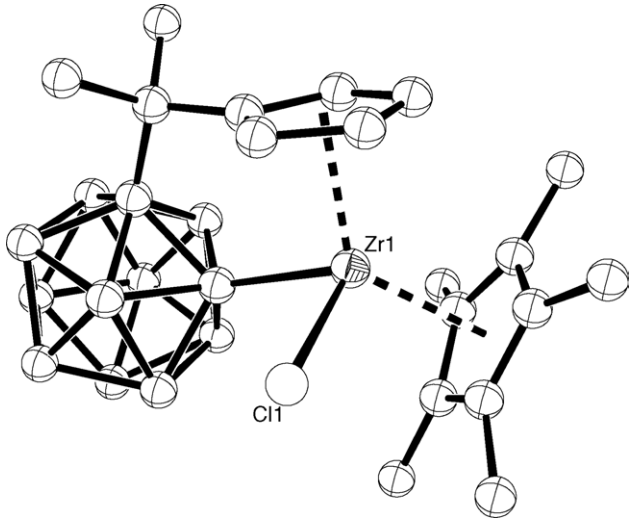

Fig. 11. Molecular structure of $(\eta^5\text{-}C_5Me_5)[\eta^5{:}\sigma\text{-}Me_2C(C_5H_4)(C_2B_{10}H_{10})]ZrCl$ [32].

cyclopentadienyl–amido ones [15,33], suggesting that carboranyl does play a role in enhancing the catalytic activity of metallocenes. Replacement of an amido unit by an icosahedral carboranyl moiety in a traditional constrained-geometry ligands of the type CpSiN can eliminate the $N(p_\pi)$-$M(d_\pi)$ back bonding interactions, thus, enhance the Lewis acidity of the central metal ion leading to the higher activity.

Metallocenes with boron-bridged ligand exhibit the highest activity among the C-, Si- and P-bridged ones, indicating that the B-linkage may have some intramolecular Lewis acid coactivations on the metal center [23]. On the other hand, the electron-rich P-linkage may decrease the Lewis acidity of the metal center, leading to a relatively lower catalytic activity [30].

The question arises as to whether the M–C (cage) bond in the above metallocenes participates in the catalysis. Since the active species were suggested to be metallocene cations containing M–CH_3 σ bond which are very difficult to be isolated, and the M–CH_3 bond is more reactive than the M–N one, $[\eta^5{:}\sigma\text{-}Me_2A(C_9H_6)(C_2B_{10}H_{10})]Zr(NMe_2)_2$ (A = C, Si) were then chosen as model complexes. Their reactions toward various unsaturated compounds were investigated in details (Scheme 11) [24]. The results clearly show that: (1) small molecules, such as CS_2, PhCN, CH_2=CHCN, ^{n}BuNCS and PhNCO inserted exclusively into the Zr–N bonds to give mono-, di-, and tri-insertion products depending upon the substrates and (2) the Zr–C (cage) bond remains intact in all reactions. It is suggested that the preference of Zr–N over Zr–C (cage) insertion is governed by steric factors. It may be concluded that the electron-deficient yet sterically hindered icosahedral carboranyl moiety can not only increase the Lewis acidity of the central metal ion leading to a higher catalytic activity, but also prevent the M–C (cage) bond from the attack of unsaturated molecules.

3. Metallocenes with linked amido(amino)–carboranyl ligands

o-Carborane is a very versatile molecule and can be converted into the *closo*-$C_2B_{10}H_{10}^{2-}$, *nido*-$C_2B_9H_{11}^{2-}$, *nido*-$C_2B_{10}H_{12}^{2-}$, and *arachno*-$C_2B_{10}H_{12}^{4-}$ under proper reaction conditions [4a]. Among these, *nido*-$C_2B_9H_{11}^{2-}$ (dicarbollide ion) is an isolobal inorganic analogue of $C_5H_5^-$ [4]. As an extension of the structural variations in Cp–D constrained-geometry ligands, the dicarbollide ion is rationally employed as a η^5 π-ligand instead of the cyclopentadienyl group in the hope that incorporation of the dicarbollide fragment into the constrained-geometry ligand framework would provide interesting opportunities for the design of met-

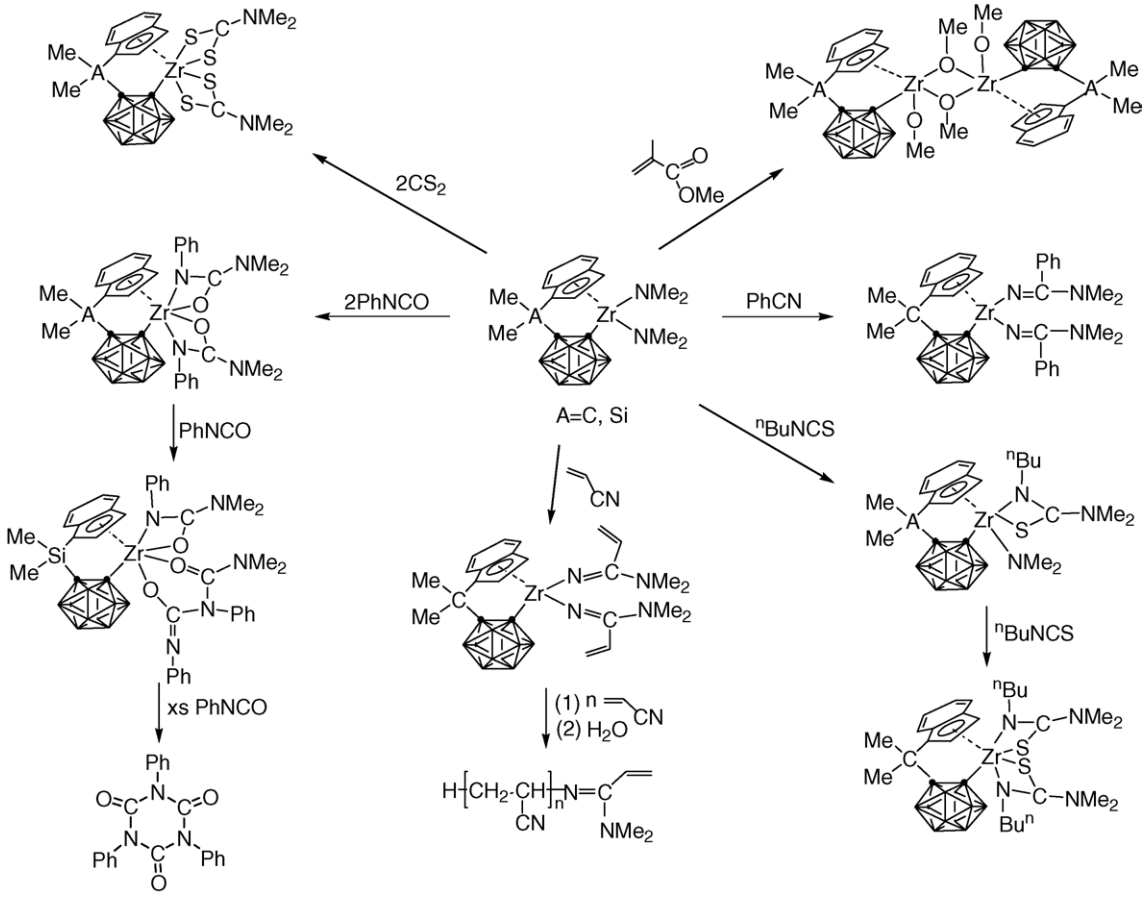

Scheme 11.

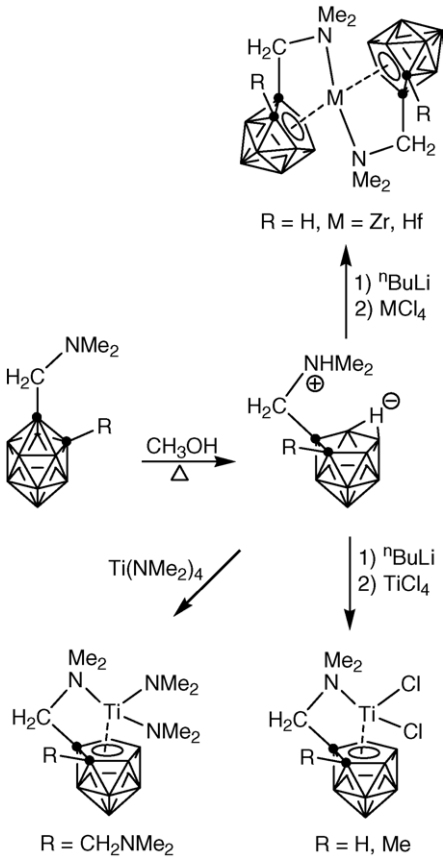

Scheme 12.

allocenes with new metal/charge combinations and increased metal unsaturation. This is a largely unexplored field and only a limited number of group 4 metal complexes with Lewis base functionalities tethered to the carborane is so far known [34–37].

Both amine elimination and salt metathesis methodologies were used to prepare the desired group 4 metal complexes. For example, treatment of $Ti(NMe_2)_4$ with one equivalent of zwitterionic salt $(Me_2NCH_2)_2C_2B_9H_{11}$ in toluene at room temperature gave $[\eta^1{:}\eta^5\text{-}(Me_2NCH_2)_2C_2B_9H_9]Ti(NMe_2)_2$ (Scheme 12) [34]. Single-crystal X-ray analyses show that only one nitrogen atom from the side arm coordinates to the Ti atom and the other stays freely, leading to a three-legged piano stool geometry (Fig. 12).

Reaction of MCl_4 with one equivalent of $[(Me_2NCH_2)RC_2B_9H_9]Li_2$ in THF at −78 °C afforded $[\eta^1{:}\eta^5\text{-}(Me_2NCH_2)RC_2B_9H_9]TiCl_2$ or $[\eta^1{:}\eta^5\text{-}(Me_2NCH_2)RC_2B_9H_9]_2M$ if M = Zr and Hf (R = H, Me) (Scheme 12) [35]. The formation of 2:1 complexes may result from the ligand redistribution reaction of the corresponding thermodynamically unstable dichloro species of Zr and Hf. The representative structure of Zr complex is shown in Fig. 13. The Zr atom is η^5-bonded to each of the two dicarbollyl rings and coordinated to two nitrogen atoms from the side arms in a distorted-tetrahedral geometry.

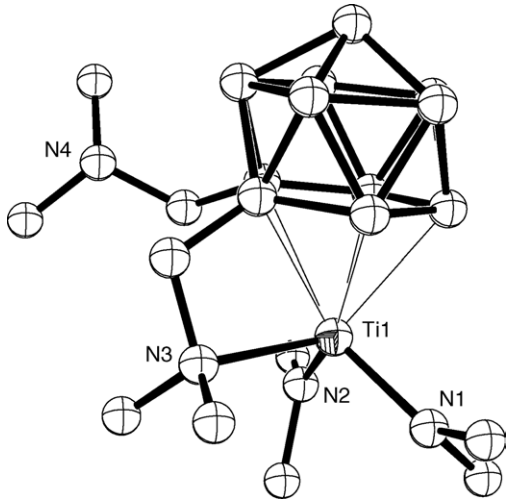

Fig. 12. Molecular structure of $[\eta^1{:}\eta^5\text{-}(Me_2NCH_2)_2C_2B_9H_9]Ti(NMe_2)_2$ [34].

Interactions of MCl_4 with the trianionic salt of $[(HNCH_2)C_2B_9H_{10}]Li_3$ in a molar ratio of 1:1 in THF at −78 °C generated $[\eta^1{:}\eta^5\text{-}(HNCH_2)C_2B_9H_{10}]MCl(THF)_n$ (M = Ti, $n = 0$; M = Zr, $n = 1$) (Scheme 13) [36]. Treatment of $[Me_2Si(NR)(C_2B_{10}H_{11})]Na_3$ with an equimolar amount of MCl_4 in THF produced $[\eta^1{:}\eta^6\text{-}Me_2Si(NR)(C_2B_{10}H_{11})]MCl(THF)_n$ (M = Ti, $n = 0$; M = Zr, $n = 1$) (Scheme 14) [37]. Their structures have not been subjected to X-ray analyses yet. The formation of M(IV) complexes is very interesting since it has been documented that MCl_4 can be easily reduced by *nido*-$R_2C_2B_{10}H_{10}^{2-}$ to give divalent species [38]. It may be assumed that the presence of the M–N σ bond could stabilize the high oxidation state of the central metal ion.

Among these complexes, only $[\eta^1{:}\eta^5\text{-}(Me_2NCH_2)RC_2B_9H_9]TiCl_2$ (R = H, Me) underwent preliminary testing for catalytic activity in ethylene polymerization using

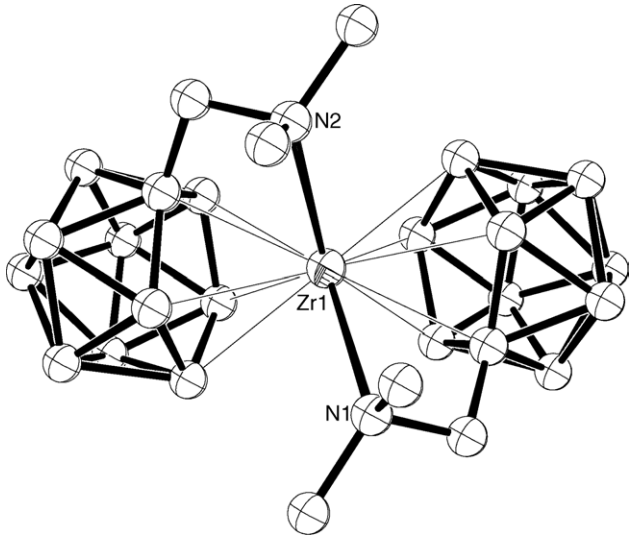

Fig. 13. Molecular structure of $[\eta^1{:}\eta^5\text{-}(Me_2NCH_2)C_2B_9H_{10}]_2Zr$ [35].

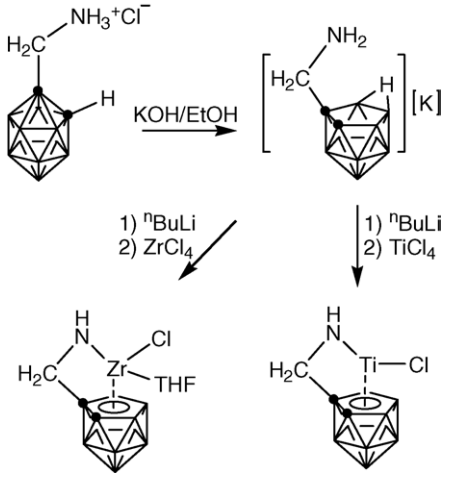

Scheme 13.

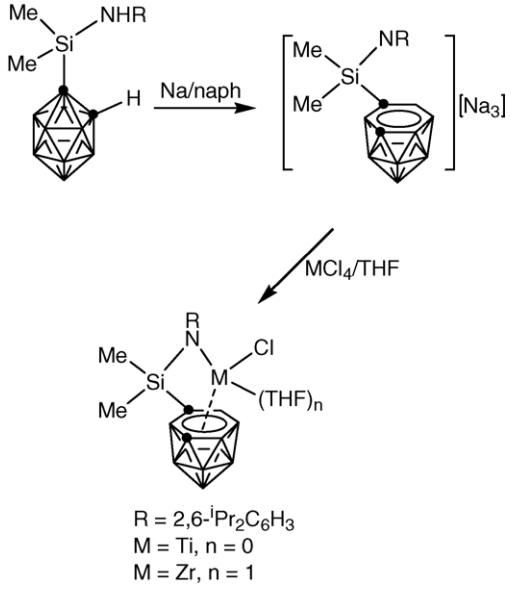

Scheme 14.

MMAO as cocatalyst (Al/Ti = 500) in hexane at 40 °C (1 atm of ethylene). The activity was 85 and 55 kg of PE $mol^{-1}\,h^{-1}\,atm^{-1}$ for R = H and Me, respectively [35].

4. Conclusions and perspectives

Many metallocenes incorporating constrained-geometry carboranyl ligands with interesting structural features have been prepared via either amine elimination or salt metathesis method. The chemistry of titanium is different from that of zirconium and hafnium in some cases probably due to the size effect.

Most of metallocenes are active catalysts for ethylene polymerization in the presence of cocatalyst (MAO, MMAO). Both the central metal ions and the linkages of the constrained-geometry ligands have a great effect on the catalytic performance of the catalysts, and the following trends are generally observed if other factors are identical: (1) $Zr \gg Ti > Hf$ and (2) $^{i}Pr_2NB > Me_2C \sim Me_2Si > {}^{i}Pr_2NP$. Zirconocenes with Me_2C- and Me_2Si-linked indenyl–carboranyl ligands are 30–100 times more active than those with R_2C- and Me_2Si-linked cyclopentadienyl–amido ones, suggesting that carboranyl does play a role in enhancing the catalytic activity of metallocenes. It is suggested that the Zr–C (cage) bond remains intact in catalysis.

In contrast, only a limited number of group 4 metal amides and chlorides with Lewis base functionalities tethered to the carborane is so far known. No metal–alkyl analogues, which are synthetic challenges in this area of chemistry, have ever been reported in the literature. Since $[\eta^1{:}\eta^5\text{-}Me_2A(NR)(C_2B_9H_{10})]MR$ (A = C, Si) is isoelectronic with Cp_2MR^+, the former may be active catalysts for polymerization/copolymerization of olefins and/or polar monomers in the absence of any cocatalysts.

The chemical properties of group 4 metal complexes incorporating linked amido(amino)–carboranyl ligands are largely unexplored and would certainly attract chemists' attention after the synthetic routes to the M–C σ bond have been realized. The search for applications of these complexes in catalysis is anticipated in the near future.

Acknowledgments

I am greatly indebted to every one of my motivated and talented graduate students and postdoc associates. Their cheerful dedication and hard work are a never-ending source of pleasure for me. I am grateful to my collaborators with whom I have had the pleasure to interact. I thank the Research Grants Council of the Hong Kong Special Administration Region, National Natural Science Foundation of China and Germany/Hong Kong Joint Research Scheme for financial support over the years.

References

[1] (a) J.A. Gladysz (Guest Ed.), Chem. Rev. 100 (4) (2000) 1167;
(b) G.J.P. Britovsek, V.C. Gibson, D.F. Wass, Angew. Chem. Int. Ed. 38 (1999) 428;
(a) W. Kaminsky, M. Arndt, Adv. Polym. Sci. 127 (1997) 144.
[2] U. Siemeling, Chem. Rev. 100 (2000) 1495.
[3] (a) K.L. Hultzsch, T.P. Spaniol, J. Okuda, Angew. Chem. Int. Ed. 38 (1999) 227;
(b) J. Park, S.C. Yoon, B.-J. Bae, W.S. Seo, I.-H. Suh, T.K. Han, J.R. Park, Organometallics 19 (2000) 1269.
[4] (a) Z. Xie, Coord. Chem. Rev. 231 (2002) 23;
(b) R.N. Grimes, in: E.W. Abel, F.G.A. Stone, G. Wilkinson (Eds.), Comprehensive Organometallic Chemistry II, vol. 1, Pergamon, NY, 1995, p. 373;
(c) A.K. Saxena, N.S. Hosmane, Chem. Rev. 93 (1993) 1081.
[5] Z. Xie, S. Wang, Z.-Y. Zhou, F. Xue, T.C.W. Mak, Organometallics 17 (1998) 489.

[6] Z. Xie, Acc. Chem. Res. 36 (2003) 1.
[7] Y. Sun, H.-S. Chan, P.H. Dixneuf, Z. Xie, Organometallics 23 (2004) 5864.
[8] Z. Xie, S. Wang, Z.-Y. Zhou, T.C.W. Mak, Organometallics 18 (1999) 1641.
[9] Z. Xie, K. Chui, Q. Yang, T.C.W. Mak, Organometallics 18 (1999) 3947.
[10] K. Chui, Q. Yang, T.C.W. Mak, Z. Xie, Organometallics 19 (2000) 1391.
[11] E. Hong, Y. Kim, Y. Do, Organometallics 17 (1998) 2933.
[12] G. Zi, Q. Yang, T.C.W. Mak, Z. Xie, Organometallics 20 (2001) 2359.
[13] M.-H. Lee, J.-W. Hwang, Y. Kim, Y. Do, Organometallics 19 (2000) 5514.
[14] S. Wang, Q. Yang, T.C.W. Mak, Z. Xie, Organometallics 19 (2000) 334.
[15] H. Wang, Y. Wang, H.-W. Li, Z. Xie, Organometallics 20 (2001) 5110.
[16] Z. Xie, S. Wang, Q. Yang, T.C.W. Mak, Organometallics 18 (1999) 2420.
[17] S. Wang, Q. Yang, T.C.W. Mak, Organometallics 18 (1999) 4478.
[18] Z. Xie, S. Wang, Q. Yang, T.C.W. Mak, Organometallics 18 (1999) 1578.
[19] S. Wang, Q. Yang, T.C.W. Mak, Z. Xie, Organometallics 18 (1999) 5511.
[20] S. Wang, H.-W. Li, Z. Xie, Organometallics 20 (2001) 3624.
[21] S. Wang, H.-W. Li, Z. Xie, Organometallics 20 (2001) 3842.
[22] G. Zi, H.-W. Li, Z. Xie, Organometallics 21 (2002) 1136.
[23] G. Zi, H.-W. Li, Z. Xie, Organometallics 21 (2002) 3850.
[24] H. Wang, H.-W. Li, Z. Xie, Organometallics 22 (2003) 4522.
[25] S. Wang, H.-W. Li, Z. Xie, Organometallics 23 (2004) 2469.
[26] S. Wang, H.-W. Li, Z. Xie, Organometallics 23 (2004) 3780.
[27] J. Wang, C. Zheng, J.A. Maguire, N.S. Hosmane, Organometallics 22 (2003) 4839.
[28] H. Wang, H. Wang, H.-W. Li, Z. Xie, Organometallics 23 (2004) 875.
[29] (a) D.W. Carpenetti, L. Kloppenburg, J.T. Kupec, J.L. Petersen, Organometallics 15 (1996) 1572;
(b) J.N. Christopher, G.M. Diamond, R.F. Jordan, Organometallics 15 (1996) 4038.
[30] H. Wang, H.-S. Chan, J. Okuda, Z. Xie, Organometallics 24 (2005).
[31] (a) G.K. Barker, M.F. Lappert, J.A.K. Howard, J. Chem. Soc. Dalton (1978) 735;
(b) J.L. Atwood, G.K. Barker, J. Holton, W.E. Hunter, M.F. Lappert, J. Am. Chem. Soc. 99 (1977) 6645.
[32] Y. Han, E. Hong, Y. Kim, K.M.H. Lee, J. Kim, J.-W. Hwang, Y. Do, J. Organomet. Chem. 679 (2003) 48.
[33] K. Kunz, G. Erker, S. Döring, S. Bredeau, G. Kehr, R. Fröhlich, Organometallics 21 (2002) 1031.
[34] Y.-J. Lee, J.-D. Lee, J. Ko, S.-H. Kim, S.O. Kang, Chem. Commun. (2003) 1364.
[35] D.-H. Kim, J.H. Won, S.-J. Kim, J. Ko, S.H. Kim, S. Cho, S.O. Kang, Organometallics 20 (2001) 4298.
[36] Y. Zhu, K. Vyakaranam, J.A. Maguire, W. Quintana, F. Teixidor, C. Viñas, N.S. Hosmane, Inorg. Chem. Commun. 4 (2001) 486.
[37] J. Wang, Y. Zhu, S. Li, C. Zheng, J.A. Maguire, N.S. Hosmane, J. Organomet. Chem. 680 (2003) 173.
[38] (a) F.Y. Lo, C.E. Strouse, K.P. Callahan, C.B. Knobler, M.F. Hawthorne, J. Am. Chem. Soc. 97 (1975) 428;
(b) C.G. Salentine, M.F. Hawthorne, Inorg. Chem. 15 (1976) 2872;
(c) W.-Y. Kwong, H.-S. Chan, Y. Tang, Z. Xie, Organometallics 23 (2004) 3098.
[39] X. Bei, C. Kreuder, D.C. Swenson, R.F. Jordan, Organometallics 17 (1998) 1085.
[40] X. Bei, V.G. Young Jr., R.F. Jordan, Organometallics 20 (2001) 355.
[41] Y. Wang, H. Wang, H. Wang, H.-S. Chan, Z. Xie, J. Organomet. Chem. 683 (2003) 39.
[42] H. Wang, H.-W. Li, X. Huang, Z. Lin, Z. Xie, Angew. Chem. Int. Ed. 42 (2003) 4347.